SIMULATION OF HIGH-SPEED CAVITATING FLOWS IN CHANNELS

I.I. Isaenko[1], A.V. Makhnov[1], E.M. Smirnov[1], A.A. Schmidt[2]

[1]Peter the Great St. Petersburg Polytechnic University, St. Petersburg, Russian Federation;

[2]Ioffe Institute of the Russian Academy of Science, St. Petersburg, Russian Federation

Cavitation is a process of vapour and gas bubbles formation in a liquid flow. It occurs when a flow pressure drops below a certain level depending on liquid's physical properties and its temperature. One of the important factors of cavitation is the presence of unsolved microscopic bubbles filled with gas and/or vapour in real liquids. These bubbles, or nucleation sites, evolve under pressure drops that are sufficient for evaporation of surrounding liquid.

A model of cavitating flows based on Euler – Lagrange description of multiphase medium has been developed. It took into account heterogeneous nature of cavitation bubbles formation. The Rayleigh – Plesset equation along with interphase mass and energy transfer equations were used to simulate bubbles evolution. The developed model provides qualitatively accurate prediction of cavity shape and its borders position in comparison with the experimental data.

Key words: high-speed flow; cavitation; Rayleigh–Plesset equation; multiphase medium

Citation: I.I. Isaenko, A.V. Makhnov, E.M. Smirnov, A.A. Schmidt, Simulation of high-speed cavitating flows in channels, St. Petersburg Polytechnical State University Journal. Physics and Mathematics. 11 (1) (2018) 41 – 49. DOI: 10.18721/JPM.11106

Introduction

Cavitation, i.e., the formation of cavities (bubbles or caverns) filled with vapor or vapor-gas mixture in a liquid is a fundamental problem that is the focus of constant interest in connection with the developing theory of multiphase media with its vast array of applications [1]. The phenomenon of cavitation occurs when pressure drops below a certain level depending on the properties of the liquid and its temperature [2 – 6]. Microscopic inclusions (such as bubbles and solid particles), i.e., nucleation sites or cavitation nuclei, that may be present in the liquid play a major role in this.

As pressure increases in the cavitating medium, cavities (bubbles) collapse, generating shock waves and high-velocity cumulative jets that cause cavitation-induced erosion.

Cavitation is a widespread phenomenon, which is why cavitation research has a great practical importance. Studies on the subject cover a diverse range of issues from physiology (for example, blood boiling with a decrease in pressure [1]) to design of power and transport equipment (water turbines, pumps, propellers, valves, etc.) [3 – 4, 7] and technologies using the effects of energy release in liquids [2, 8 – 9].

The erosion accompanying the evolving cavitation can greatly affect the functioning of the corresponding devices, decreasing their productivity and even causing them to break down. Therefore, erosion research is also of great interest in fundamental and applied research.

It should be noted that experimental study of cavitation is incredibly difficult due to the extreme values of cavitation parameters and different spatio-temporal scales of the processes under consideration. Because of this, mathematical modeling becomes a promising and effective tool for studying cavitation [7 – 9].

This paper is devoted to the analysis of one possible approach to mathematical simulation of cavitation.

Mathematical model of cavitating fluid flows

The Euler/Euler and Euler/Lagrange representations [10] are the two main approaches to flow simulation in multiphase media.

In the first case, the heterogeneous medium under consideration is replaced by a quasi-homogeneous mixture with continuous distributions of densities, velocities, pressures, and other phase parameters. Both phases (carrier liquid and bubbles) in this model occupy the entire volume of the mixture, and the concept of phase volume fraction is introduced, allowing to determine the effective densities of the components of a quasi-homogeneous mixture and to use a system of Navier – Stokes equations for computing cavitation flows.

However, these models typically do not account for the physics of evolution of the bubbles formed during cavitation, which can be a crucial factor in some cases.

Within the second approach, the motion of the carrier phase is governed by the equations of dynamics of a continuous medium, and the Lagrange approach based on introducing a set of test particles is used for describing the motion of dispersed phase (in particular, bubbles). The computation of flows in a multiphase medium includes the following stages:

solving the carrier phase equations (Euler stage);

solving the equations of test particle motion in accordance with the flow field of the carrier phase obtained in the previous stage (the Lagrange stage equations);

solving the interphase transport equations to take into account the effect of the dispersed phase on the carrier;

refining the flow field of the carrier phase taking into account the effect of the dispersed phase (a new time step within the Euler stage).

The second approach involves considerable computational costs but allows to compute the dynamics of each test particle (bubble) individually, and also to take into account the fact that the particle size distribution is non-uniform, in contrast with the Euler/Euler model that averages the particles' behavior. This advantage is the reason why developing Euler/Lagrange methods seems to be the most expedient.

The motion of the carrier phase at the Euler stage is described by a system of Navier – Stokes equations:

$$\frac{\partial \rho}{\partial t} + \nabla \cdot (\rho \mathbf{V}) = 0;$$

$$\frac{\partial (\rho \mathbf{V})}{\partial t} + \nabla \cdot (\rho \mathbf{V}\mathbf{V}) = -\nabla P + \frac{\partial \tau_{ij}}{\partial x_j}; \qquad (1)$$

$$\frac{\partial}{\partial t}(\alpha_v \rho_v) + \nabla \cdot (\alpha_v \rho_v \mathbf{V}) = S_v - S_l,$$

where ρ, kg/m^3 is the mixture density; $\rho = \rho_l \alpha_l + \rho_v \alpha_v$, ($\alpha$ is the volume fraction of matter, the indices l and v refer to liquid and vapor, respectively); $\mathbf{V}$, m/s, is the velocity vector; P, Pa, is the pressure; S, kg/m^3·s, are the source terms (distribution densities of mass sources, the indices l and v also refer to liquid and vapor, respectively); τ_{ij} are the stress tensor components.

The motion of bubbles in the velocity field at the Lagrange stage is computed with or without mass forces:

$$\frac{d\mathbf{X}}{dt} = \mathbf{F}, \qquad (2)$$

where $\mathbf{X} = [x; y; z]$, $\mathbf{F} = [V_x; V_y; V_z]$ (V_i are the velocity components).

Next, a system of equations based on the laws of conservation of mass and energy is solved:

$$\frac{d}{dt}\left(\frac{4}{3}\pi R_B^3 \rho_v\right) = 4\pi R_B^2 \dot{m}, \qquad (3)$$

$$\frac{d}{dt}\left(\frac{4}{3}\pi R_B^3 \rho_v U_B\right) = -P_B \frac{d}{dt}\left(\frac{4}{3}\pi R_B^3\right) - 4\pi R_B^2 U_{12}, \qquad (4)$$

where R_B is the radius of a cavitation bubble; m is the mass; U_B is the internal energy of a cavitation bubble; P_B, Pa, is the vapor pressure in a cavitation bubble; U_{12} is the energy flux through the interface.

System (3), (4) can be transformed to the following form, suitable for directly determining the parameters of the vapor inside the bubble [9, 19]:

$$\frac{dP_B}{dt} = P_B\left(\frac{1}{T_B}\frac{dT_B}{dt} - \frac{3}{R_B}\left[\frac{dR_B}{dt} - \frac{\eta_{ac}T_B}{P_B}\frac{\sqrt{r_v}}{\sqrt{2\pi}}\left(\frac{P_s(T_l)}{\sqrt{T_l}} - \frac{P_B}{\sqrt{T_B}}\right)\right]\right); \quad (5)$$

$$\frac{dT_B}{dt} = -3\frac{T_B}{R_B P_B}\left[(\gamma-1)\left(P_B + \frac{2\Sigma}{R_B}\right)\frac{dR_B}{dt} + \eta_{ac}P_s(T_l)(T_B - T_l)\sqrt{\frac{r_v}{2\pi T_l}}\right], \quad (6)$$

where P_s, Pa, is the saturated vapor pressure; T_l, T_B, K, are the temperatures of liquid and gas in the bubble, respectively; η_{ac} is the accommodation coefficient; r_v is the specific gas constant; Σ, N/m, is the coefficient of surface tension; γ is the adiabatic exponent of gas.

The accommodation coefficient η_{ac} is equal to 0.04 for water, the specific gas constant $r_v = P_v/\rho_v T_v M_v$ (T_v is the vapor temperature, M_v is the molar mass of the gas in the bubble), the adiabatic exponent of gas $\gamma = 1.4$.

Eqs. (5) and (6) are supplemented by the equation for the dynamics of radial motion of a bubble in the Rayleigh – Plesset form [11, 12]:

$$R_B\frac{d^2R_B}{dt^2} + \frac{3}{2}\left(\frac{dR_B}{dt}\right)^2 = \frac{1}{\rho_l}\left(P_B - P_\infty - \frac{4\mu}{R_B}\frac{dR_B}{dt} - \frac{2\Sigma}{R_B}\right), \quad (7)$$

where P_∞, Pa, is the external flow pressure; μ, Pa·s, is the dynamic viscosity.

This equation describes the growth and collapse of a spherically symmetric vapor bubble taking into account the inertia in the radial motion of the surrounding liquid, the difference between internal and external pressures ($P_B - P_\infty$), and viscosity and surface tension. The processes of gas diffusion have not been described in our study.

Approaches to describing the emerging cavitation

Most models of cavitation flows use the Euler/Euler description of a two-phase medium. They can be based on barotropic equations of the state of the medium [18], thermodynamic relations [17] or the coupling equations between the source terms S responsible for interphase mass transfer and the dynamics of bubble growth and collapse [16, 17]. The problem of flow past a NACA-66 airfoil was considered in [13, 14, 16], with experimental data provided in [15].

A number of cavitation models based on thermodynamic relations for phase transitions were proposed in [17]. The simplest of these models is based on the assumption of phase equilibrium and the number of cavitation nuclei sufficient to neglect the metastable state time, which is valid for simple flows. The study also considers some more complex differential models that take into account metastability, heat transfer during phase transitions, presence of bubbles of undissolved gas and other factors. Models using the Euler/Euler description give qualitatively similar distributions of the vapor fraction and are adequate for predicting the size of the cavities. However, these models do not take into account the physics of vaporization and condensation, since they assume that vapor is formed only when the saturation pressure is reached (the volume fraction of gas bubbles in the mixture is assumed to be sufficient to neglect the delay in the phase transition). Another disadvantage of this approach is that the simulation results depend on the values of empirical parameters included in the equations; because of this, they have to be additionally adjusted [16, 17].

In recent years, various research groups have performed computations of cavitation flows using the Euler/Lagrange description. In Ref. [19], a cavitation cloud was computed using the Lagrange method for modeling the dynamics of discrete bubbles. The carrier phase is represented by a quasi-homogeneous mixture with a variable continuous density distribution satisfying the laws of conservation of mass and momentum. The growth and collapse of bubbles was simulated using the Keller – Herring equation (a modification of the Rayleigh – Plessset equation). The volume fraction of vapor was computed from the data on the location of bubbles and their sizes, a Gaussian distribution function was used to

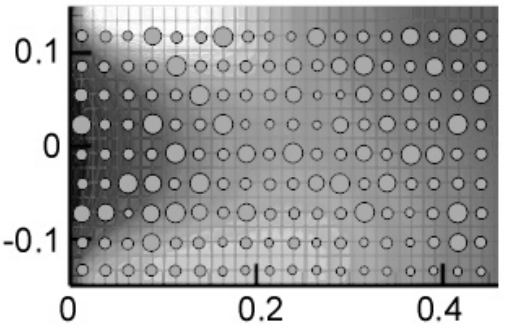

Fig. 1. Computational scheme for the distribution of test bubbles in the field of the carrier medium based on the experimental data of [4]

convert the discrete distribution of bubbles in the volume to a continuous density field of the mixture.

These studies used the data on the microparticles (microbubbles) observed in liquids, serving as nucleation sites. According to the experimental data of Ref. [4], one cubic meter of distilled water contains about $10^{11} - 10^{12}$ nucleation sites, and their characteristic radii lie in the range from 1 to 6 μm (Fig. 1). The presence of these sites ensures that heterogeneous nucleation evolves and cavitation bubbles develop [20]. The basis for the developing cavitation nuclei are the particles or surface inhomogeneities whose sizes (radii) exceed the critical value R_{cr}, determined from the Laplace relation:

$$R_{cr} = \frac{2\Sigma}{P_s - P_l}, \qquad (8)$$

where the indices s and l refer, respectively, to saturated vapor pressure and pressure in the liquid flow.

In this study we have used a technique for computing cavitation flows based on the Euler/Lagrange description of a two-phase medium and a simplified model of heterogeneous nucleation in which only vapor bubbles present in the liquid act as vaporization centers (other factors, such as air bubbles, solid impurities and surface roughness were not taken into account).

The Euler/Lagrange algorithm for computation of cavitating media flow

Each time step within the Euler stage of the algorithm involves determining the velocity and pressure fields of the carrier medium, used as input data for the Lagrange stage. At the first step, the computational domain is filled with test bubbles (see Fig. 1).

The initial distribution of bubbles in the liquid in this study is given in accordance with the experimental data from [4]. The size distribution of nucleation sites is replaced by a piecewise constant function; N_B is the number of nuclei with a radius R_B (Fig. 2).

The Lagrange stage of the algorithm

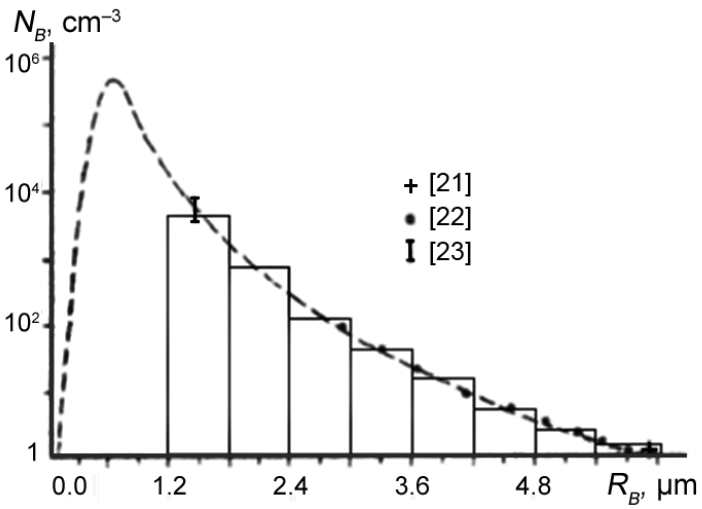

Fig. 2. Approximation of the spectrum of nucleation sites (dashed line) by a piecewise constant function (solid lines)

involves computing the motion and the change in the size of the test bubbles. In this case, the fields of the carrier phase are interpolated according to the scheme shown in Fig. 3, *a* to determine the parameters in the location of the bubble. The growth of test bubbles is described by system of equations (5) – (7).

After all available test bubbles have been processed, the volume fraction of vapor is computed taking into account the number of bubbles in each control volume and the numerical density (the probability of finding the bubbles) is computed for bubbles of a given type per unit volume (reference volume). The scheme used translates the values from bubble locations to the nearest nodes of the auxiliary computational grid (Fig. 3, *b*). This approach ensures that the field of the vapor volume fraction is continuous. The density field is adjusted with respect to the obtained values of the vapor volume fraction; next, adjustments for taking into account the law of conservation of mass are introduced, and a transition to the Euler stage is made for a new physical time step.

When bubbles move and grow, they can interact with each other and merge. The merging and break-off of bubbles is not taken into account in our study. Instead, a conditional boundary, determined by the value of the vapor volume fraction α_v, is introduced between bubble cavitation and cavity modes. In the latter case, Euler/Euler description can be used in the region where cavitation is deemed to be well-developed (with high α_v values) and the internal parameters of the bubbles are fixed. Such a hybrid model preserves the advantages of the Lagrange description of the dynamics of discrete bubbles in cases of bubbly cavitation and allows to avoid time-consuming computations of the parameters of each bubble in regions with well-developed cavitation.

The assumptions introduced make it possible to simplify the implementation of the method, since that way, it is no longer necessary to simulate cavity collapse and the merging of individual bubbles, keeping their number constant. In this case, the cavity is represented by an artificial dense 'cloud' of cavitation bubbles.

Testing the model

The following problems have been considered in simulating the cavitation process:

1. Evolution of a single bubble with sinusoidal oscillations of fluid pressure (acoustic cavitation):

$$P(t) = P_0 + (P_{\max} - |P_{\min}|)\sin(2\pi t/t_{per}), \quad (9)$$

where P_0, $P_{\max}$, $P_{\min}$ are the mean, maximum and minimum pressures; t_{per} is the period of pressure oscillations.

2. The flow in a narrow channel of variable cross-section (Fig. 4); the channel considered

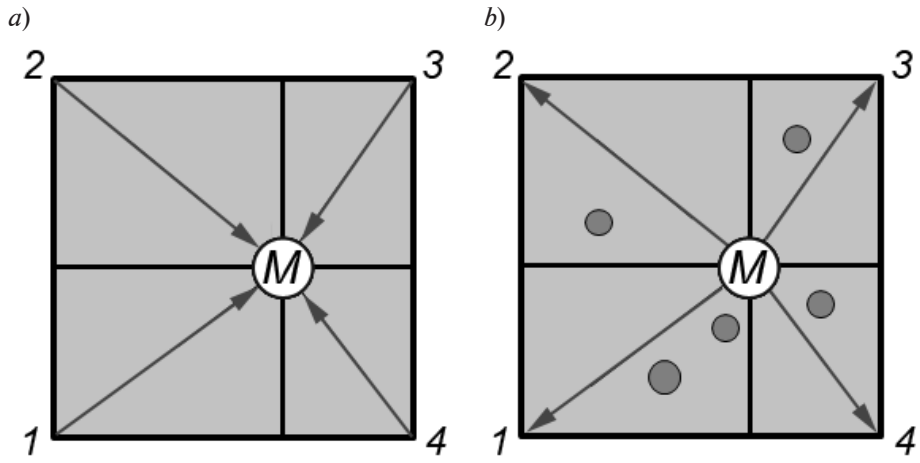

Fig. 3. Schematic explaining the connection between the Lagrange and the Euler stages of the computational algorithm:
a is the interpolation of hydrodynamic variables from grid nodes *1 – 4* to the location of bubble *M*, *b* is the transfer of information about the vapor fraction to grid nodes *1 – 4*

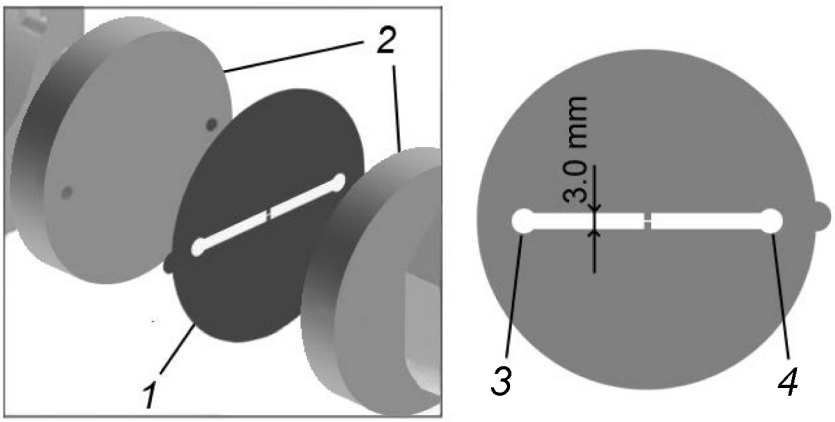

Fig. 4. Experimental setup for simulating the flow in the injector [7]:
plate with a channel *1*, windows for supply and discharge of liquid *2*, channel inlet *3*, input pressure P_{in} = 300 atm, channel outlet *4*, outlet pressure P_{out} = 52 atm

is the same as the one described in [7].

Applying the Euler/Lagrange description involves a number of difficulties in this case. One of them is the problem of spatial scales: the characteristic sizes of the computational cells are comparable to the sizes of the cavitation bubbles, so it is necessary either to introduce additional coarsened grids or to construct special schemes for taking into account the effect of bubble distribution. The number of bubbles per unit volume may be less than one for the scales considered; the quantity should then express the probability of finding a bubble in a given (control) volume.

We have carried out the Euler stage of numerical solution using solvers that are part of the OpenFOAM computing environment; the Lagrange stage was carried out using a specially developed software module.

The curves in Fig. 5 illustrate the growth of a single bubble with an initial radius R_B = 2 μm at an amplitude of pressure fluctuations ΔP = 200 atm and at different temperatures of the medium. It can be seen that the collapsing bubbles resume growth at the time of the second pressure drop. The differences in temperatures

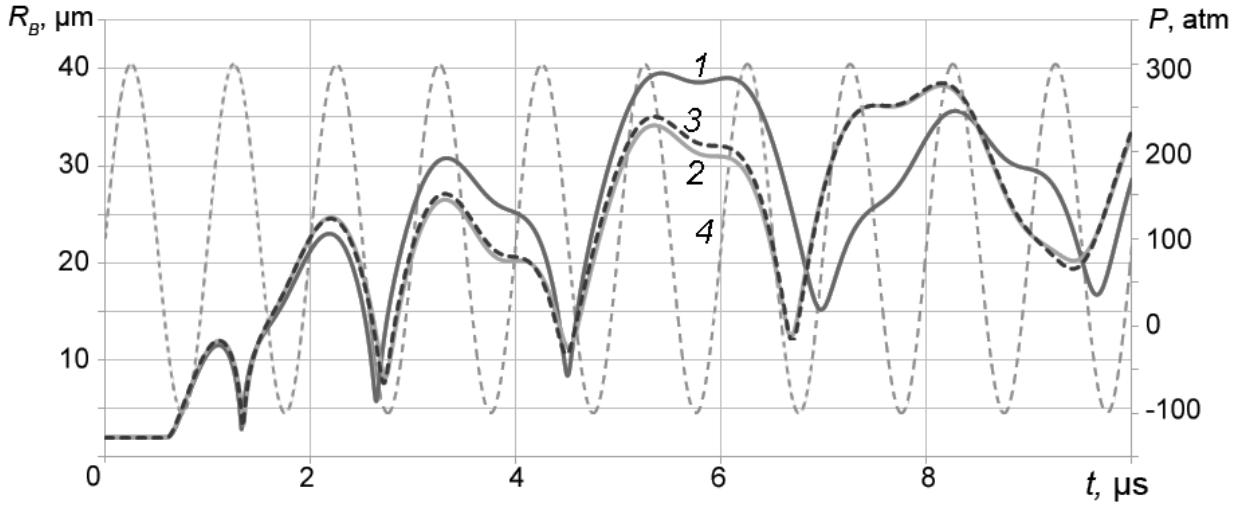

Fig. 5. Growth dynamics of a single bubble at different temperatures of the medium, °C:
30 (curve *1*), 60 (*2*), 90 (*3*); the variations in the pressure of the medium are given (curve *4*).
The initial bubble radius is 2 μm

of the carrier medium have a pronounced effect if we compare the computational data at temperatures of 30 °C and above 60 °C. Bubbles start to grow earlier at higher temperatures, so respectively, they gain relatively larger mass and inertia, and their collapse occurs with a delay. For this reason, growth then also resumes with a delay, and as a result, the bubbles in the more heated liquid grow to a smaller volume than at a temperature of 30 °C at the time of the third increase in pressure. Further dynamics is governed by two main factors: the inertia of the bubble and the fluctuations in the external pressure. Notice that this effect is not observed in the computations with the single Rayleigh – Plesset equation: the bubble disappears after the first period of pressure recovery.

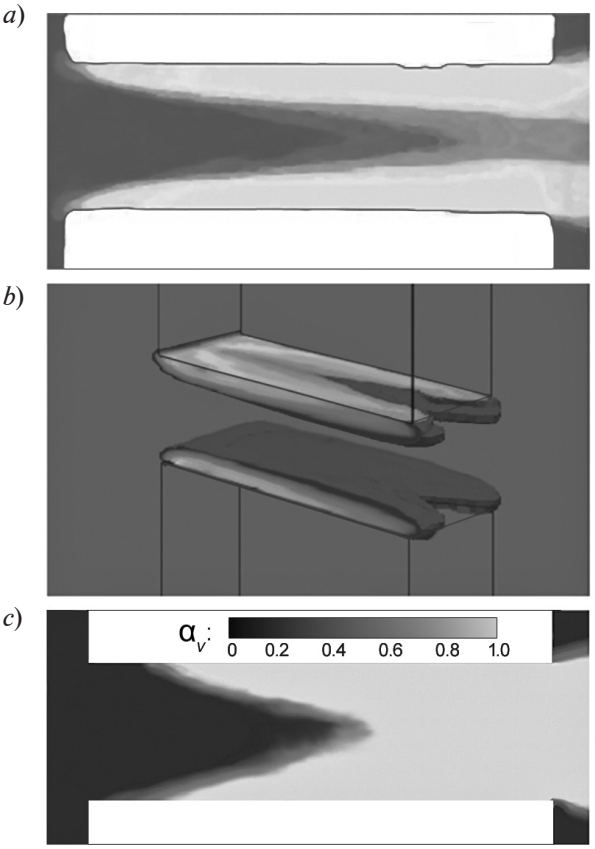

Fig. 6. Cavity shapes obtained experimentally (*a*) and from the computations (*b*, *c*).
Experimental data [7] are given for the time when the cavity extended beyond the channel (t = 60 μs), T = 326 K, P_{out} = 52 atm. The results of model flow computations were obtained in accordance with the Euler/Euler (*b*) and Lagrange/Euler (*c*) descriptions

Thus, it is more important to take into account the change in internal parameters at the stage of bubble collapse than at the stage of growth, where, according to our results, the dynamic behavior of the process does not significantly depend on the model used for describing it.

The conclusions drawn about the applicability of various equations of bubble dynamics allow to compile a scheme for computing more complex problems of cavitation flows. The changes in the internal parameters of the bubble can be neglected in the computations during the initial expansion of bubbles and the formation of cavities, because taking these parameters into account does not make a significant contribution to bubble growth dynamics at this stage.

Thus, the following states of the test bubble have been considered within the framework of this model:

cavitation nucleus;
primary growth of the bubble;
part of the cavity region;
collapsing bubble;
bubble ceasing to exist either as a result of collapse, collision with the wall or extending beyond the computational domain.

Fig. 6 shows a comparison of the obtained distribution of the volume fraction of vapor at time t = 60 μs with the results of computations using the cavitatingFoam solver and with the averaged experimental data presented in [7]. Even though the results obtained by the Euler/Lagrange method of simulating the test bubble dynamics turn out to be somewhat overestimated, they are closer to the averaged experimental results [7]. In both cases, the cavity extends beyond the narrow part of the channel. The vaporization rate is underestimated in the computations by the Euler/Euler approach due to the peculiarities of the model.

Conclusion

In this paper, we have formulated a model of cavitation flow including the evolution of cavitation bubbles. We have used the Euler/Lagrange description of the medium taking into account a heterogeneous mechanism of bubble formation. Bubble growth and collapse

were simulated using the Rayleigh–Plesset equation and the equations of interphase mass and energy transfer determining the internal parameters of the bubbles.

The developed model ensures qualitative agreement of the cavity's shape and the position of its trailing boundary with the experimental observations.

REFERENCES

[1] **I.S. Pearsall,** Cavitation. UK: Mills and Boon, 1972.

[2] **V.K. Kedrinskiy,** Gidrodinamika vzryva. Eksperiment i modeli [Explosion hydrodynamics. Experiment and models], Novosibirsk, the RAS Siberian Branch, 2000.

[3] **Ya.E. Geguzin,** Puzyri [Bubbles], Moscow, Nauka, 1985.

[4] **A.D. Pernik,** Problemy kavitatsii [Cavitation problems], Leningrad, Sudostroyeniye, 1966.

[5] **R.T. Knapp, J.W. Daily, F.G. Hammitt,** Cavitation, McGraw-Hill, 1970.

[6] **J.-P. Franc, J.-M. Michel,** Fundamentals of cavitation, Dordrecht, Kluwer Academic Publishers, 2004.

[7] **R. Skoda, U. Iben, A. Morozov, et al.,** Numerical simulation of collapse induced shock dynamics for the prediction of the geometry, pressure and temperature impact on the cavitation erosion in microchannels, WIMRC 3rd International Cavitation Forum, 2011, University of Warwick, UK.

[8] **N.V. Petrov, A.A. Schmidt,** Effect of a bubble nucleation model on cavitating flow structure in rarefaction wave, Shock Waves. 27 (4) (2017) 635–639.

[9] **N.V. Petrov, A.A. Schmidt,** Multiphase phenomena in underwater explosion, Exp. Therm. Fluid Sci. 60 (2015) 367–373.

[10] **A. Sokolichin, G. Eigenberger, A. Lapin, A. Lübert,** Dynamic numerical simulation of gas-liquid two-phase flows: Euler/Euler versus Euler/Lagrange, Chemical Eng. Science. 52 (4) (1997) 611–626.

[11] **Lord Rayleigh,** VIII. On the pressure developed in a liquid during the collapse of a spherical cavity, Philosophical Magazine, Ser. 6. 34 (200) (1917) 94–98.

[12] **M. Plesset, A. Prosperetti,** Bubble dynamics and cavitation, Ann. Rev. Fluid Mech. 9 (1977) 145–185.

[13] **S. Frikha, O. Coutier-Delgosha, J.A. Astolfi,** Influence of the cavitation model on the simulation of cloud cavitation on 2D foil section, Int. Journal of Rotating Machinery. 2008 (2008), ID 146234, 12 p.

[14] **A.A. Gavrilov, A.A. Dekterev, K.A. Finnikov,** Modelirovaniye kavitatsionnykh techeniy s ispolzovaniyem RANS podkhoda [Cavity flows simulation using RANS approach], Proceedings of the 4-th Russian National Conf. on Heat Exchange (RNCHE-4), Moscow, 5 (2006) 241–244.

[15] **Y. Shen, P. Dimotakis,** The influence of surface cavitation on hydrodynamic forces, Proceedings of the 22nd American Towing Tank Conference, St. John's, Canada, August (1989) 44–53.

[16] **F. Bakir, R. Rey, A.G. Gerber, et al.,** Numerical and experimental investigations of the cavitating behavior of an inducer, International Journal of Rotating Machinery. 10 (1) (2004) 15–25.

[17] **U. Iben,** Modeling of cavitation; Systems Analysis, Modeling and Simulation (SAMS). 42 (2002) 1283–1307.

[18] **D.P. Schmidt, C.J. Rutland, M.L. Corradini,** A fully compressible, two-dimensional model of small, high-speed, cavitating nozzles, Atomization and Sprays. 9 (3) (1999) 255–276.

[19] **J. Ma, C.-T. Hsiao, G.L. Chahine,** Shared-memory parallelization for two-way coupled Euler–Lagrange modeling of cavitating bubbly flows, J. Fluids Engineering. 137 (4) (2015) 121106-1–121106-8.

[20] **E.Yu. Kumzerova, A.A. Schmidt,** Numerical simulation of homogeneous nucleation and bubble dynamics in a depressurized liquid, Proc. 4th International Conference on Multiphase Flow. New Orleans (2001).

[21] **M. Strasberg,** Undissolved air in cavitation nuclei, Cavitation in Hydrodynamics. London: National Phys. Lab., 1956.

[22] **F.G. Hammitt**, **A. Koller**, **O. Ahmed, et al.,** Cavitation threshold and superheat in various fluids, Proc. of Conference on Cavitation. Edinburg, September 3-5 (1974) 341–354.

[23] **A.S. Besov, V.K. Kedrinskii, E.I. Pal'chikov,** Izucheniye nachalnoy stadii kavitatsii s pomoshchyu difraktsionnoy opticheskoy metodiki [Studying of initial stage of cavitation using diffraction-optic method], Tech. Phys. Letters. 10 (4) 1984. 240–244.

Received 29.09.2017, accepted 09.11.2017.

THE AUTHORS

ISAENKO Iliya I.
Peter the Great St. Petersburg Polytechnic University
29 Politechnicheskaya St., St. Petersburg, 195251, Russian Federation
a906nn@gmail.com

MAKHNOV Andrey V.
Peter the Great St. Petersburg Polytechnic University
29 Politechnicheskaya St., St. Petersburg, 195251, Russian Federation
a_makhnov@mail.ru

SMIRNOV Evgeniy M.
Peter the Great St. Petersburg Polytechnic University
29 Politechnicheskaya St., St. Petersburg, 195251, Russian Federation
smirnov_em@spbstu.ru

SCHMIDT Alexander A.
Ioffe Institute of RAS, Peter the Great St. Petersburg Polytechnic University
26 Politechnicheskaya St., St. Petersburg, 194021, Russian Federation
alexander.schmidt@mail.ioffe.ru